Electronic Supplementary Material (ESI) for Dalton Transactions.
This journal is © The Royal Society of Chemistry 2018

Supporting Information File

3D isomorphous lanthanide coordination polymers displaying magnetic refrigeration, slow magnetic relaxation and tunable proton conduction

Siba Prasad Bera, Arpan Mondal, Subhadip Roy, Bijoy Dey, Atanu Santra, Sanjit Konar*

Department of Chemistry, Indian Institute of Science Education and Research Bhopal, Bhopal Bypass Road, Bhauri, Bhopal 462 066, India. E-mail: skonar@iiserb.ac.in; Fax: +91-755-6692392; Tel: +91-755-6691313.

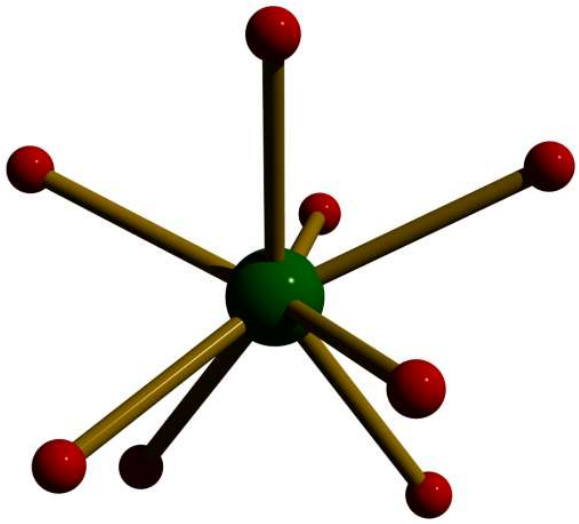

Fig. S1 Coordination environment of Er^{3+}found in CP **4** (Color codes: Er (deep green) and O (red).

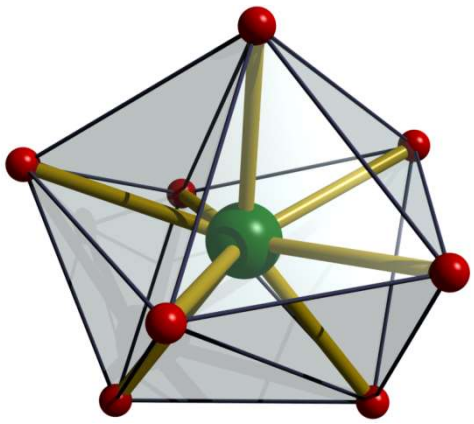

Fig. S2 Polyhedral view of Triangular dodecahedron coordination geometry of Erbium ion found in CP **4.**

Table S1. Summary of SHAPE analysis around Ln^{3+} center of CPs.

OP-8	1	D_{8h}	Octagon
HPY-8	2	C_{7v}	Heptagonal pyramid
HBPY-8	3	D_{6h}	Hexagonal bipyramid
CU-8	4	O_h	Cube
SAPR-8	5	D_{4d}	Square antiprism
TDD-8	6	D_{2d}	Triangular dodecahedron
JGBF-8	7	D_{2d}	Johnson gyrobifastigium J26
JETBPY-8	8	D_{3h}	Johnson elongated triangular bipyramid J14
JBTPR-8	9	C_{2v}	Biaugmentedtrigonal prism J50
BTPR-8	10	C_{2v}	Biaugmentedtrigonal prism
JSD-8	11	D_{2d}	Snub diphenoid J84
TT-8	12	T_d	Triakis tetrahedron
ETBPY-8	13	D_{3h}	Elongated trigonalbipyramid

$[ML_8]$	OPY-8	HPY-8	HBPY-8	CU-8	SAPR-8	TDD-8	JGBF-8	JETBPY-8	JBTPR-8	BTPR-8	JSD-8	TT-8	ETBPY-8
Gd1	30.191	21.824	15.245	9.508	1.850	**0.805**	14.708	26.444	2.486	2.028	2.806	10.134	22.557
Dy1	30.509	22.329	14.427	10.288	1.550	**0.796**	13.353	27.556	1.933	1.254	3.931	11.080	23.156
Ho1	30.226	21.581	15.533	9.842	1.780	**0.892**	14.451	26.406	2.416	1.939	2.848	10.464	22.640
Er1	30.286	21.478	15.570	9.887	1.810	**0.931**	14.413	26.286	2.374	1.940	2.829	10.476	22.541

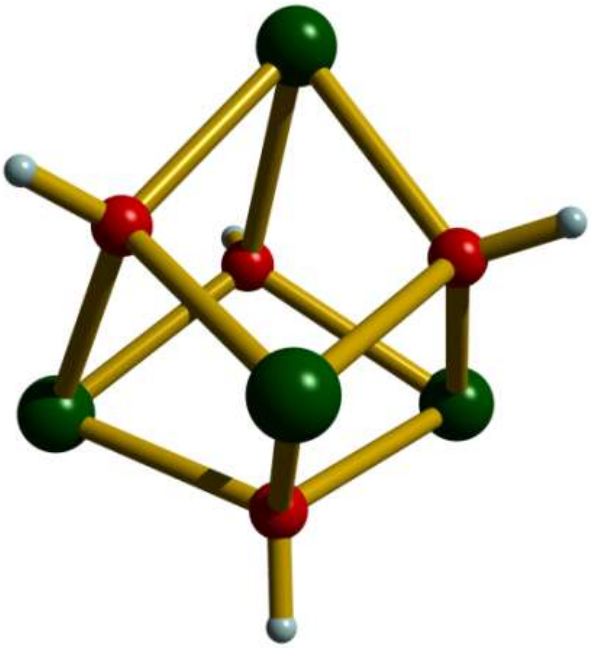

Fig. S3 Distorted cubic unit in CP **4.**

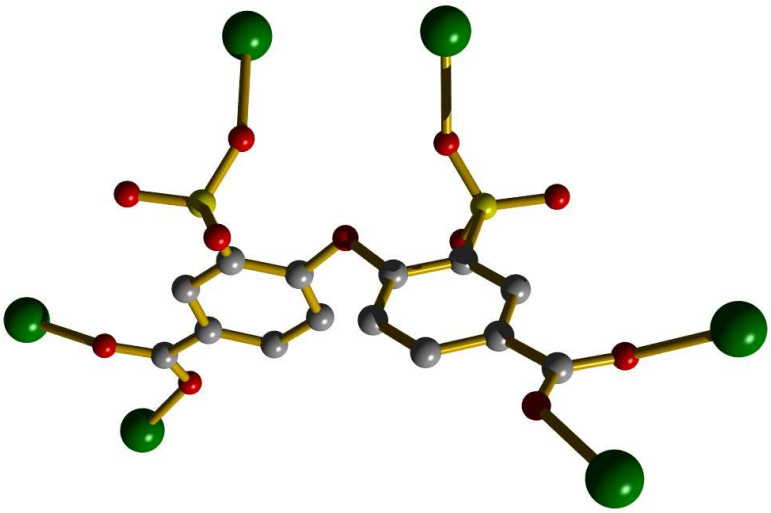

Fig. S4 View of coordination modes of ligand with lanthanide ions.

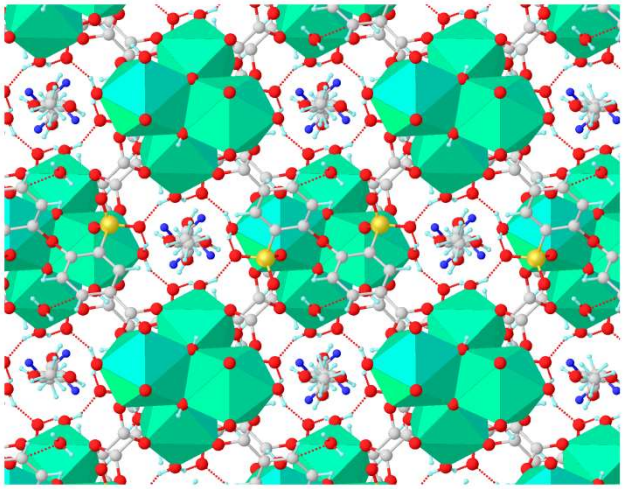

Fig. S5 Illustration H-bonding interaction in the channels in CPs along crystallographic *c*-axis

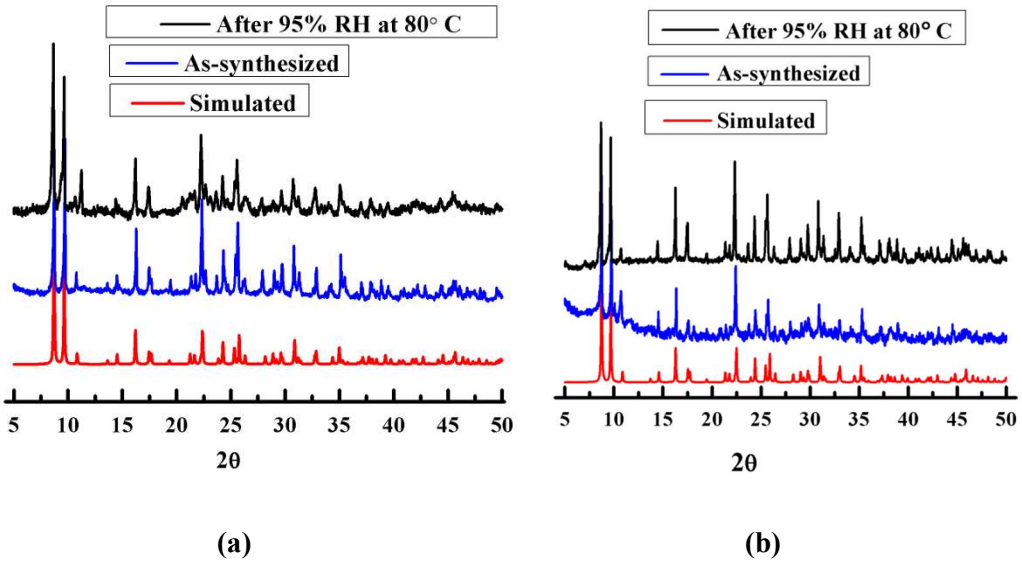

Fig. S6 PXRD pattern of (a) CP **1** and (b) CP **2**

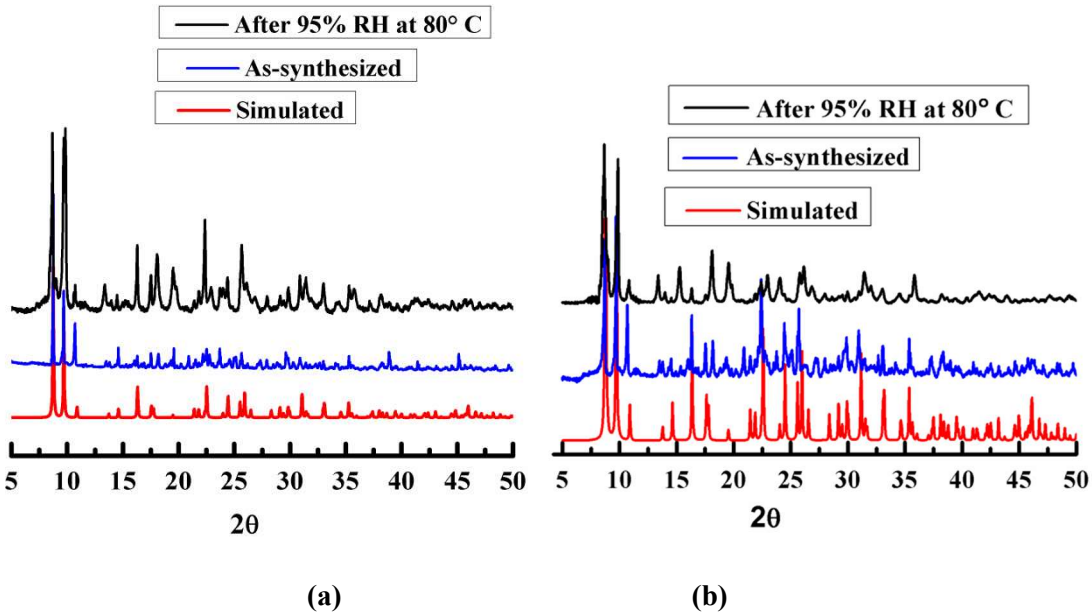

Fig. S7 PXRD pattern of (a) CP **3** and (b) CP **4**

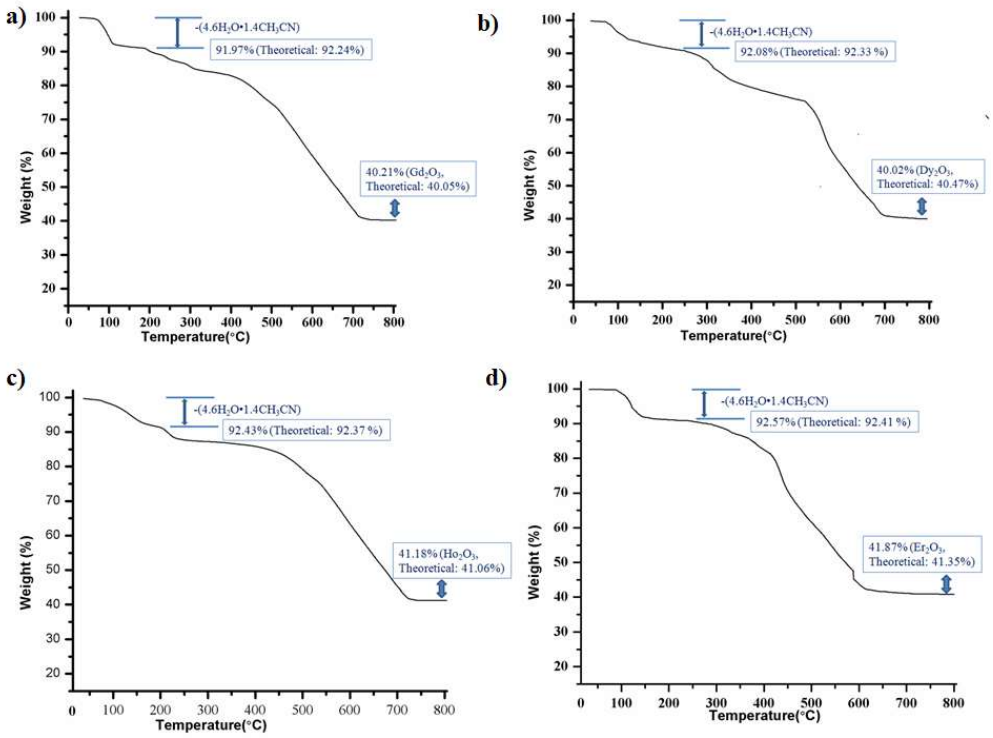

Fig. S8 Thermogravimetric plots of CPs **1-4** (a -d)

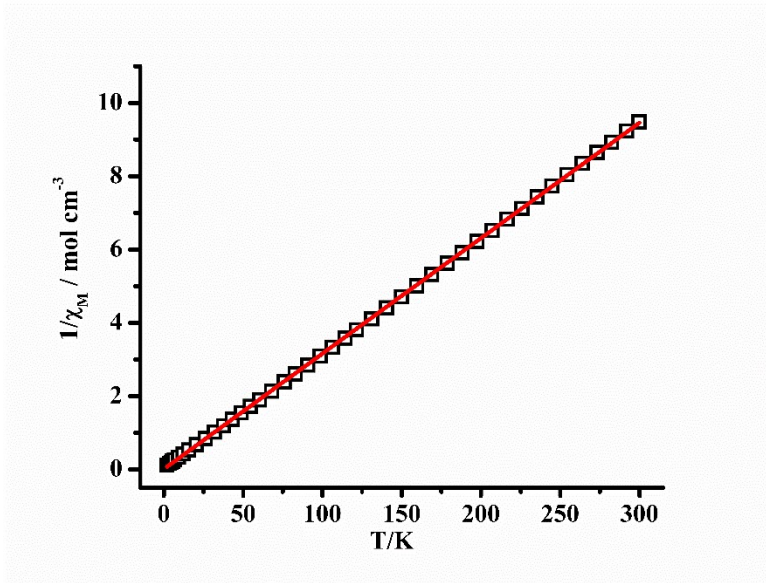

Fig. S9 Curie–Weiss fitting plot for CP **1**.

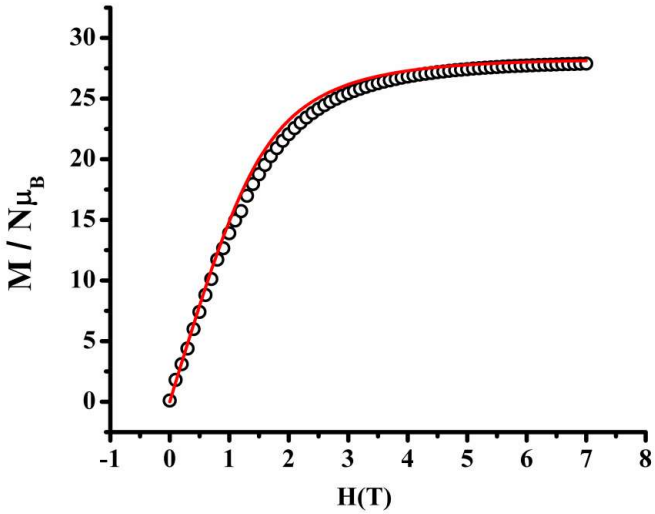

Fig. S10 Fitting plot of the magnetization data for CP **1**.

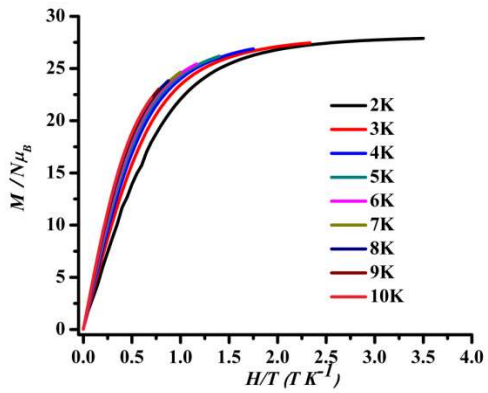

Fig. S11 Isothermal normalized magnetizations vs. field/temperature plot for CP **1** collected for temperatures ranging from 2 to 10 K.

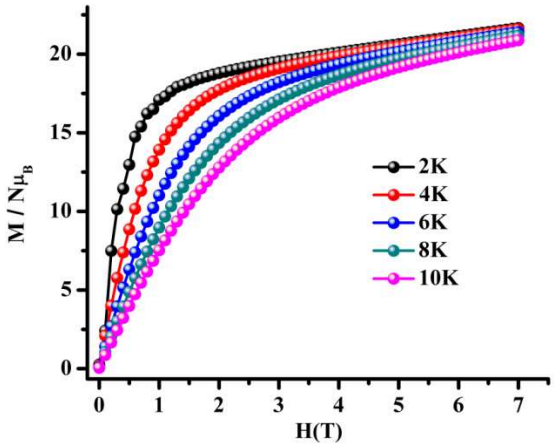

Figure S12. Magnetization plot for CP **2**.

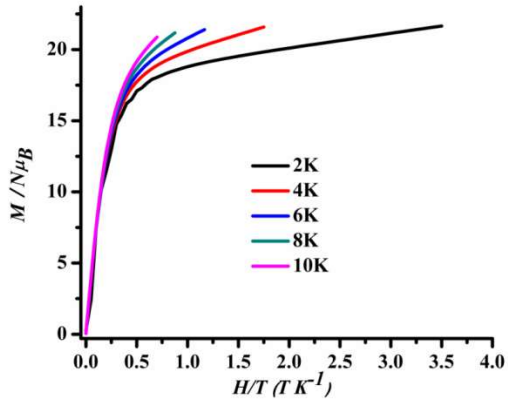

Fig. S13 Isothermal normalized magnetizations vs. field/temperature plot for CP **2** collected for temperatures ranging from 2 to 10 K.

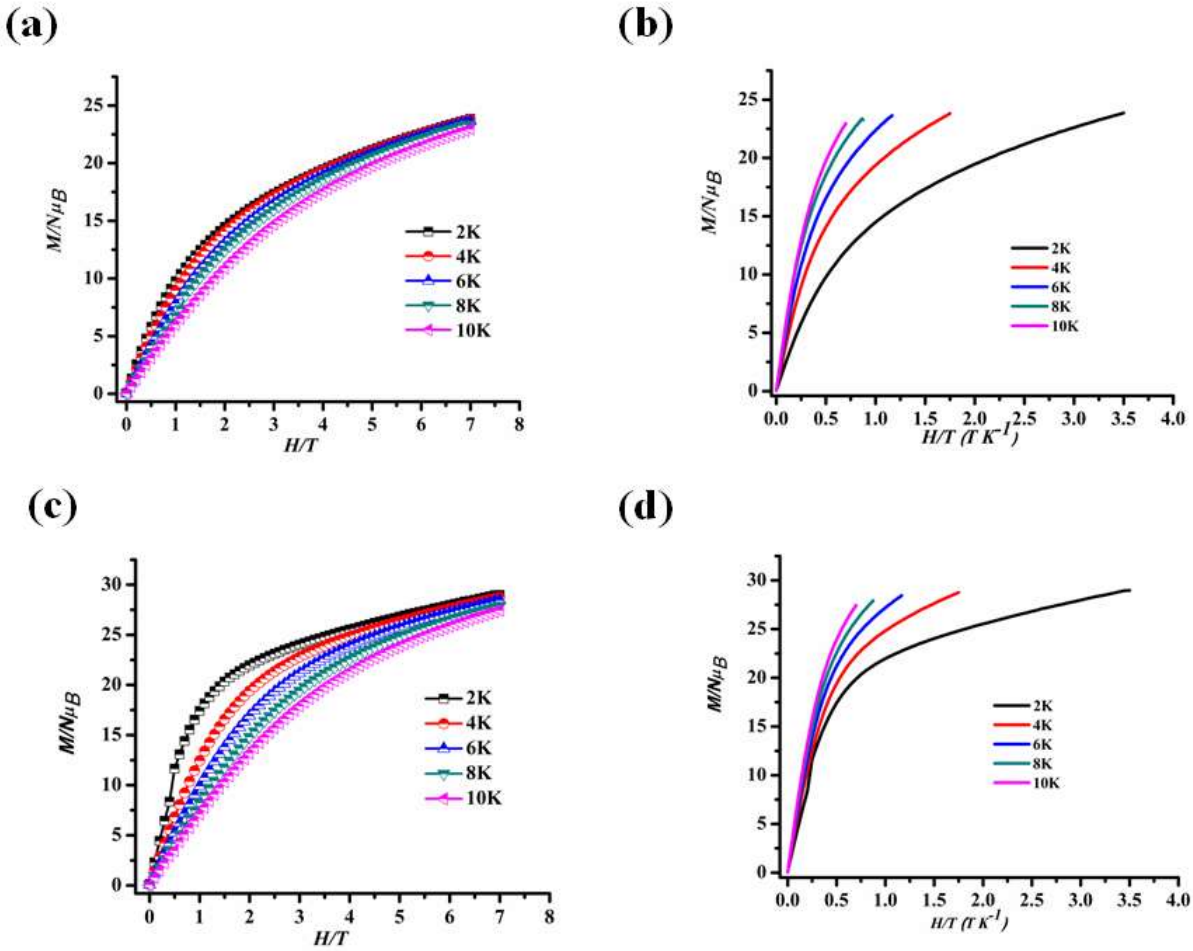

Fig. S14 Magnetization and Isothermal normalized magnetizations vs. field/temperature for CP **3** (a and b) and CP **4** (c and d)

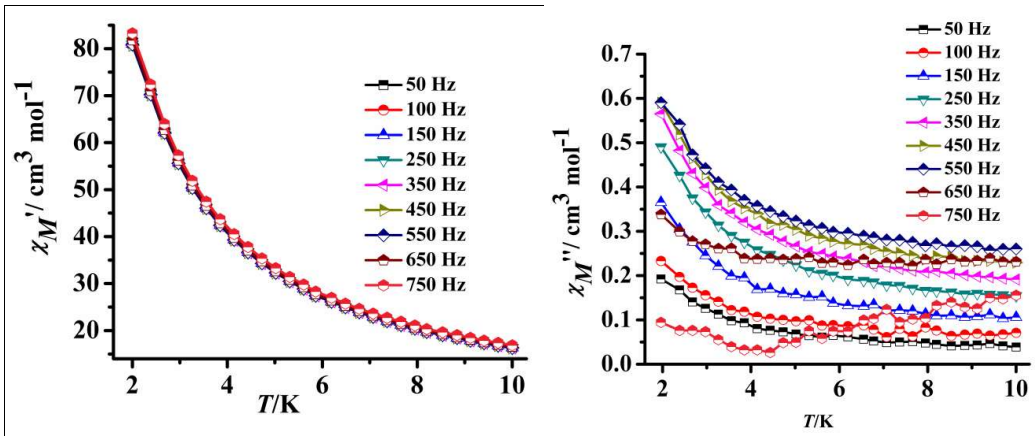

(a) (b)

Fig. S15 (a) Temperature dependence of the in phase (χ') and (b) out of phase (χ'') ac susceptibility components for **CP 2** at the indicated frequencies and in 0 Oe DC field

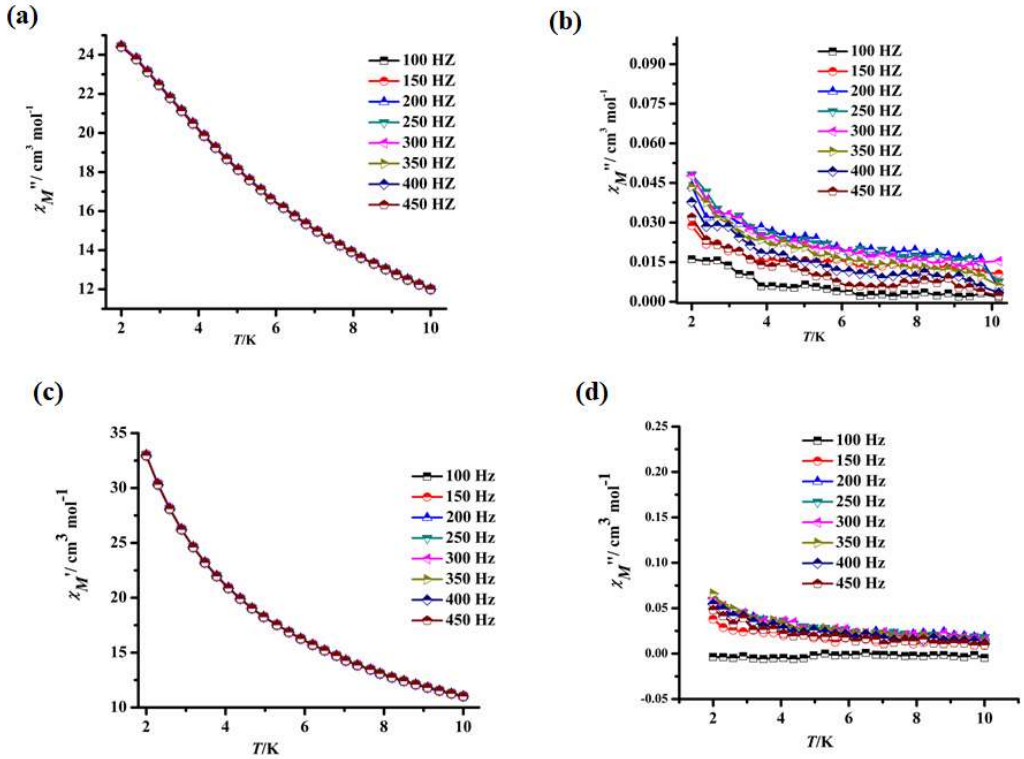

Fig. S16 (a) Temperature dependence of the in phase (χ') and (b) out of phase (χ'') ac susceptibility components for CP **3** and (c) temperature dependence of the in phase (χ') and (d) out of phase (χ'') ac susceptibility for CP **4** at the indicated frequencies and in 0 Oe DC field

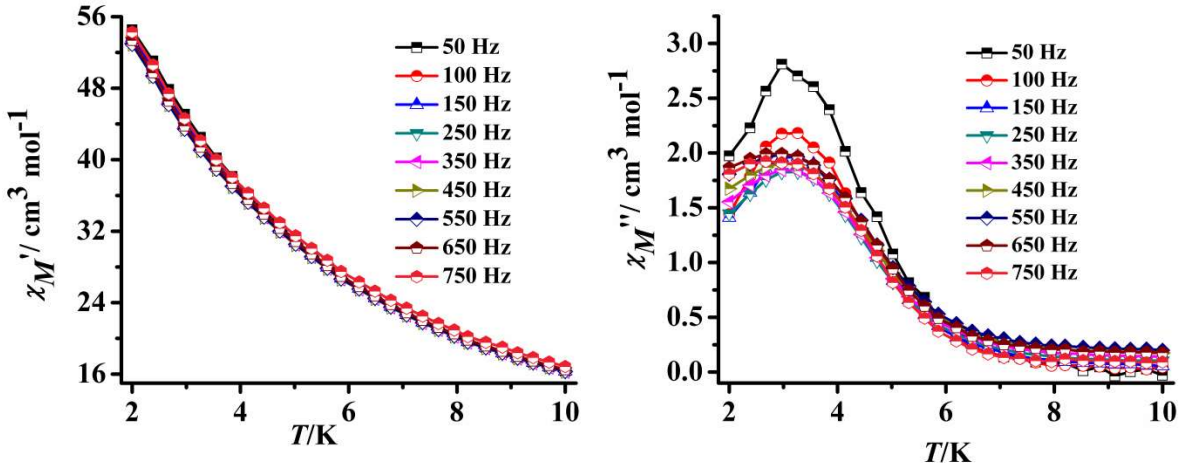

(a) (b)

Fig. S17 (a) Temperature dependence of the in phase (χ') and (b) out of phase (χ'') ac susceptibility components for CP **2** at the indicated frequencies and in 1000 Oe DC field

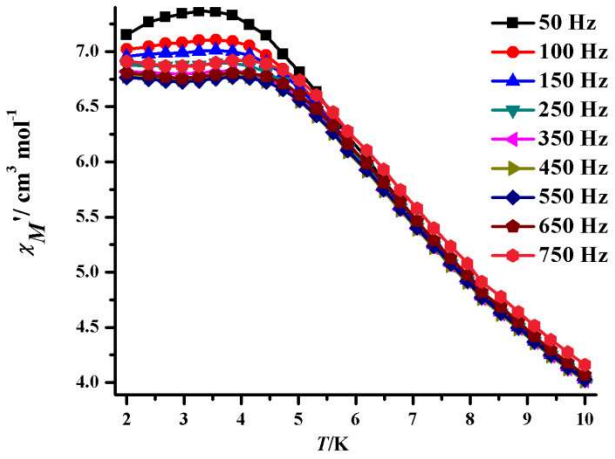

Fig. S18 Temperature dependence of the in phase (χ') ac susceptibility components for CP **2** at the indicated frequencies and in 2000 Oe DC field.

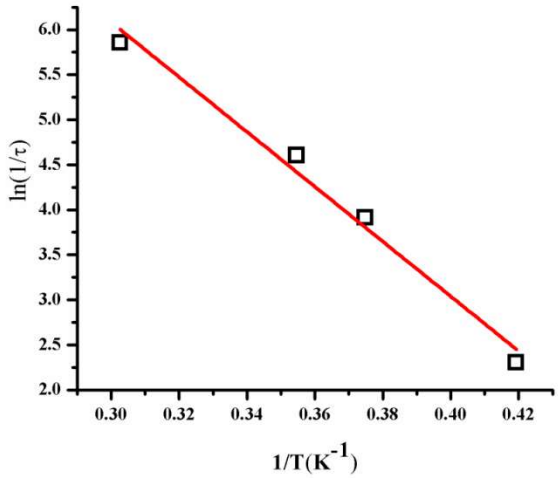

Fig. S19 Arrhenius plot for complex CP **2** to calculate anisotropic energy barrier and magnetic relaxation time.

Computational Methods: All the calculations were performed on the geometry extracted from the experimental X-ray data and the Gd(III) center is replaced by Lu(III). The DFT calculations were performed with the ORCA 4.0 software package. The hybrid B3LYP functional has been used to calculate the isotopic exchange constant by comparing the energies of high spin (HS) and broken-symmetry (BS) spin states. Also the relativistic effects were included with the zero order regular approximation (ZORA), together with the scalar relativistic contracted version of the basis functions def2-TZVP for Gd, Lu, S, and O atoms and def2-SVP for C and H atoms. We have also used the chain-of-spheres approximation (RIJCOSX) to exact exchange.

The *ab initio* calculations of CP2 were performed with MOLCAS 8.2 software package. For all the atoms ANO-RCC basis set of function were used as [ANO-RCC...8s7p5d3f2g1h.] for Dy, [ANO-RCC...8s7p5d3f2g1h.] for Lu, [ANO-RCC...4s3p1d.] for S, [ANO-RCC...3s2p1d.] for O, [ANO-RCC...3s2p.] for C and [ANO-RCC...2s.] for H, including the relativistic effects within Douglas Kroll Hess Hamiltonian.[(a) M. Douglas, N. M. Kroll, *Ann. Phys.,* 1974, **82**, 89-155; (b) B. A. Hess, *Phys. Rev. A,* 1986, **33**, 3742-3748. (c) M. Reiher, *WIREs Comput. Mol. Sci.,* 2012, **2**, 139-149.] To save the disk space the Cholesky decomposition for two electrons integral is employed throughout the calculations. We have included nine electrons in seven metal based 'f' orbitals, CAS (9, 7) in the active space of CASSCF calculations and 21 sextets in the RASSCF method. The RASSI-SO program [P. Å. Malmqvist, B. O. Roos, B. Schimmelpfennig, *Chem. Phys. Lett.* 2002**, 357**, 230-240.] has been used to include the spin orbit coupling in the 21 sextets optimized in the previous calculations. The SINGLE_ANISO module [L. F. Chibotaru, L. Ungur, *J. Chem. Phys. 2012*, **137**, 064112.] was used to calculate the energy, the transition matrix element between the KDs and relevant information.

Table S2. Computed *g* tensor and energy level of all 8 KDs

Sr. No.	g_{xx}	g_{yy}	g_{zz}	Energy (cm^{-1})
1	0.090	0.310	18.82	0.00
2	1.677	3.25	14.09	54.14
3	2.95	5.67	8.64	90.76
4	0.82	4.66	10.07	137.32
5	1.19	4.94	11.63	178.08
6	11.16	7.50	2.57	200.21
7	0.24	0.41	18.56	271.84
8	0.01	0.01	19.72	422.22

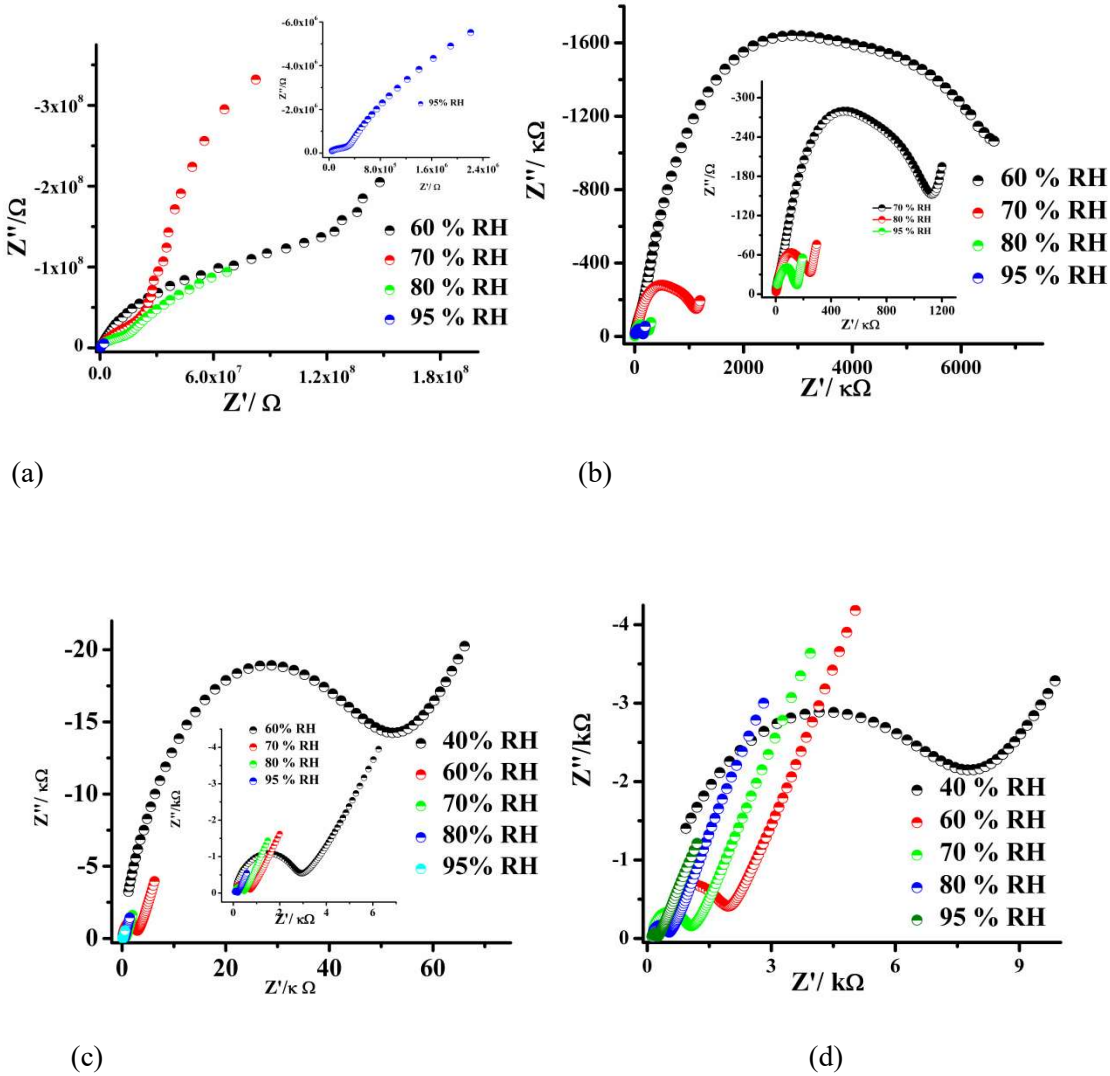

Fig. S20 Nyquist plots of complex CPs: (a) for CP **1**, (b) for CP **2** ,(c) for CP **3** and(d) for CP **4)**. at 30˚ C and different RH.

Table S3. Comparison of Proton Conductivity of sulfonate group containing coordination polymers or CPs / MOFs at specified condition

CPs or MOF	Ligand	Structural features / guest	σ / S cm^{-1}	RH %	T (°C)	Ref.
$[Er_4(OH)_4(L)_2(H_2O)_8]$•4.6$H_2O$•1.4$CH_3CN\}_n$	disodium-2,2′-disulfonate-4,4'-oxydibenzoic acid	non-coordinating sulfonate oxygen atoms, aqua ligands line channels / lattice water, acetonitrile	6.59 x10^{-3}	95	80	This work (CP **4**)
$\{[Ln_4(OH)_4(L)_2(H_2O)_8]$•4.6$H_2O$•1.4$CH_3CN\}_n$	disodium-2,2′-disulfonate-4,4'-oxydibenzoic acid	non-coordinating sulfonate oxygen atoms, aqua ligands line channels / lattice water, acetonitrile	4.56 x10^{-3}	95	80	This work (CP **3**)
CuH(Hspip)(HPO_4)·H_2O	2-sulfophenylimidazo(4,5-f)(1,10)-phenanthroline	non-coordinating sulfonate oxygen atoms, coordinated Cl^{-1} HPO_4^{2-} groups/ guest H_2O	6.90 × 10^{-4}	97	95	4.(a)
TMOF-1	disodium 1,2 ethanedisulfonate, 4,40 – bipyridine	non-coordinating sulfonate oxygen atoms	1.62 ×10^{-6}	98	90	4.(b)
TMOF-2	1,4 benzenedimethanesulfonate, 4,40 -bipyridine	non-coordinating sulfonate oxygen atoms, aqua ligands	1.23 ×10^{-4}	98	90	4.(b)
Tb-DSOA	disodium-2,2′-disulfonate-4,4'-oxydibenzoic acid	non-coordinating sulfonate oxygen atoms, aqua ligands line channels / lattice water	1.7×10^{-4}	98	100	4.(d)
Zn(5-sipH)-(bpy)].DMF .2H_2O	5-sulfoisophthalic acid and 4,4’-bipyridine	non-coordinating sulfonic acid groups on the pore surface / DMF and water	3.9×10^{-4}	60	25	4.(g)
[Zn(H2O)(5-sipH)-$(bpe)_{0.5}$]. DMF	5-sulfoisophthalic acid and 1,2-di(4-pyridyl)ethyrene	non-coordinating sulfonic acid groups on the pore surface / DMF	3.4×10^{-8}	60	25	4.(g)
$[Zn_3(5\text{-}sip)_2$(5-sipH)(bpy)].(DMF).2(DMA)	5-sulfoisophthalic acid and 4,4’-bipyridine	non-coordinating sulfonic acid groups on the pore surface / DMF and DMA	8.7×10^{-5}	60	25	4.(g)
β-PCMOF2	trisodium 2,4,6-trihydroxy-1,3,5-trisulfonate benzene	Oxygen atoms from SO_3^- groups line channels / lattice water	1.3×10^{-3}	90	85	4.(h)

$PCMOF2_{1/2}$	trisodium 2,4,6- trihydroxy-1,3,5-trisulfonate benzene and 1,3,5-benzenetriphosphonic acid	Oxygen atoms from SO_3^-, PO_3^{2-} groups line channels / lattice water	2.1×10^{-2}	90	85	4.(h)
Nafion	Polymer namely perfluorosulfonic membranes	-	10^{-2}	98	20-80	4.(k)
Sr-SBBA	4,4'-sulfobisbenzoic acid	Sulfone group in backbone facilitate Hbonding	4.4×10^{-5}	98	25	4.(l)

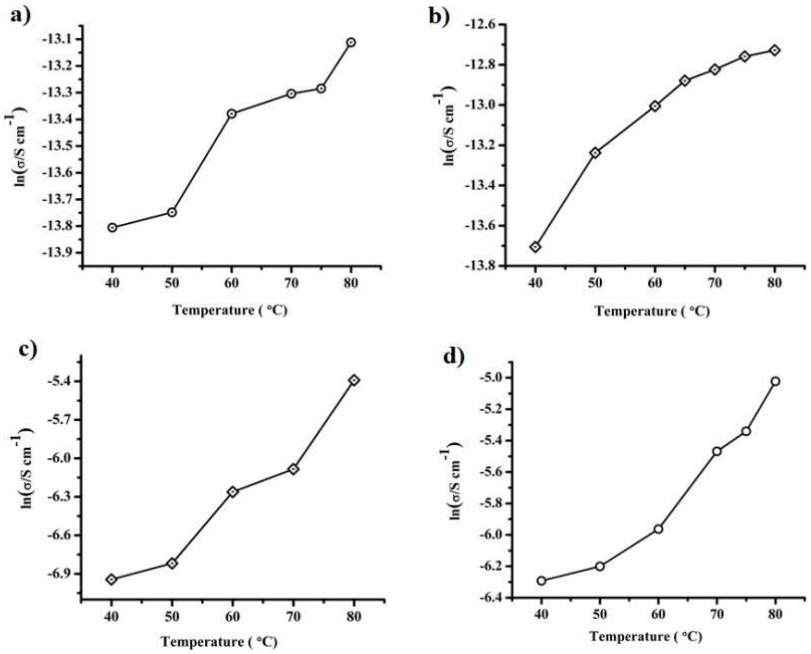

Fig. S21 Temperature dependencies of proton conductivity of coordination polymers ((a), (b), (c) and (d) for CP **1,** CP **2,** CP **3** and CP **4** respectively) at 95% RH.

Details of the simulation of the water vapor adsorption of CP 4

After removing the lattice solvent molecules through squzee, a new cif. file was generated and the file was imported to Sorption module of the Material Studio 6.1 version to locate the adsorbed water molecules at 80°C.We run the moduleby using COMPASS27 forcefield. The used summation methode is Ewald. The program run at constant temperature. MetropolisMonte Carlo method is used here.

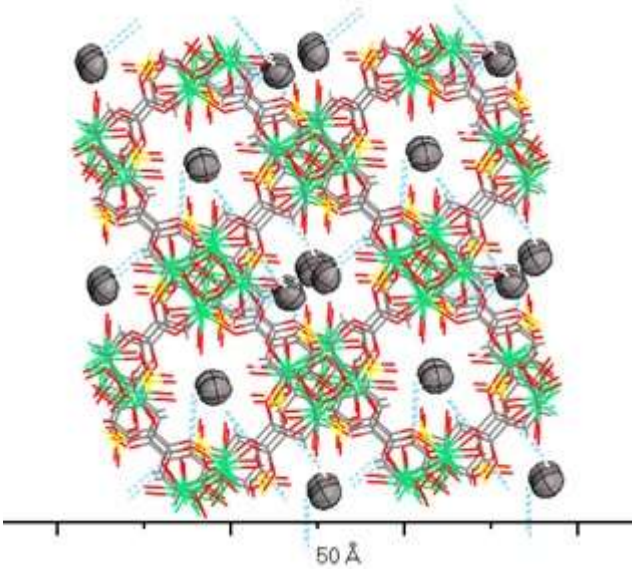

Fig. S22 Packing view of adsorbed water molecule in the channel (simulated)

Table S4. X-Ray Crystallographic Data and Refinement Parameters for CPs.

	CP 1	**CP 2**	**CP 3**	**CP 4**
Formula	$C_{30.8}H_{45.4}Gd_4N_{1.4}O_{38.6}S_4$	$C_{30.8}H_{45.4}Dy_4N_{1.4}O_{38.6}S_4$	$C_{30.8}H_{45.4}Ho_4N_{1.4}O_{38.6}S_4$	$C_{30.8}H_{45.4}Er_4N_{1.4}O_{38.6}S_4$
M_w (g mol^{-1})	1810.12	1831.12	1840.84	1850.16
Crystal system	Tetragonal	Tetragonal	Tetragonal	Tetragonal
Space group	*I*-4	*I*-4	*I*-4	*I*-4
T (K)	139.0	120	296.15	296.15
a (Å)	12.9717(5)	12.8964(4)	12.8759(6)	12.8363(2)
b (Å)	12.9717(5)	12.8964(4)	12.8759(6)	12.8363(2)
c (Å)	16.3190(7)	16.2519(6)	16.2369(7)	16.2028(4)
α (°)	90	90	90	90
β (°)	90	90	90	90
γ (°)	90	90	90	90
V (Å^3)	2745.9(2)	2703.0(2)	2691.9(3)	2669.75(11)
Z	2	2	2	2
ρ_{calcd} (g cm^{-3})	2.189	2.250	2.271	2.302

μ(MoKα) (mm^{-1})	5.025	5.726	6.077	6.487
F(000)	1738.0	1754.0	1762.0	1770.0
Collected reflections	22321	8591	7832	9888
Unique reflections	4010	3557	3441	3819
Goodness-of-fit (GOF) on F^2	1.061	0.918	1.004	1.018
R1, (I > 2σI[a]	0.0180	0.0166	0.0201	0.0216
wR2, (I > 2σI)[a]	0.0389	0.0338	0.0395	0.0406
CCDC Number	1838574	1838575	1838576	1838577

[a] $R_1 = \Sigma||F_o| - |F_c||/\Sigma|F_o|$ and $wR_2 = |\Sigma w(|F_o|^2 - |F_c|^2)|/\Sigma|w(F_o)^2|^{1/2}$

Table S5. Relevant bond distances (Å) for CPs.

CP**1**		CP**2**		CP **3**		CP **4**	
Gd1- O1	2.383(3)	Dy1-O1	2.344(3)	Ho1- O1	2.353(3)	Er1- O1	2.329(3)
Gd1- O1^1	2.470(3)	Dy1- O1^1	2.440(3)	Ho1- O1^1	2.435(3)	Er1- O1^1	2.418(3)
Gd1- O1^2	2.409(3)	Dy1- O1^2	2.374(2)	Ho1- O1^2	2.380(3)	Er1- O1^2	2.362(4)
Gd1- O3^3	2.352(3)	Dy1- O3^3	2.315(3)	Ho1- O3^3	2.319(4)	Er1- O3^3	2.296(4)
Gd1- O2L	2.499(3)	Dy1- O2L	2.466(4)	Ho1- O2L	2.471(4)	Er1- O2L	2.450(4)
Gd1- O2	2.342(3)	Dy1- O2	2.314(3)	Ho1- O2	2.315(4)	Er1- O2	2.290(4)
Gd1- O1L	2.448(3)	Dy1- O1L	2.403(3)	Ho1- O1L	2.405(4)	Er1- O1L	2.387(4)

CP **1**:^{1}-1-x,-y,+z; ^{2}-1/2-y,1/2+x,-1/2-z; ^{3}-1/2+y,-1/2-x,-1/2-z; ^{4}-1-y,1+x,-1-z; ^{5}-2-x,-1-y,+z

CP **2**: ^{1}-1-x,-y,+z; ^{2}-1/2-y,1/2+x,-1/2-z; ^{3}-1/2+y,-1/2-x,-1/2-z; ^{4}-1-y,1+x,-1-z; ^{5}-2-x,-1-y,+z

CP **3**:^{1}1-x,-y,+z; ^{2}1/2-y,-1/2+x,1/2-z; ^{3}1/2+y,1/2-x,1/2-z; ^{4}1-y,-1+x,1-z; ^{5}2-x,1-y,+z

CP **4**:^{1}1-x,-y,+z; ^{2}1/2-y,-1/2+x,1/2-z; ^{3}1/2+y,1/2-x,1/2-z; ^{4}1-y,-1+x,1-z; ^{5}2-x,1-y,+z

Table S6. Relevant bond angles (°) around the metal centers found in **CPs**

CP**1**

Atom	Atom	Atom	Angle/°	Atom	Atom	Atom	Angle/°
O1	Gd1	O1^1	72.34(11)	Gd1	O1	Gd1^4	104.94(10)
O1	Gd1	O1^2	66.64(11)	Gd1^4	O1	Gd1^2	102.31(10)
O1^1	Gd1	O1^2	70.84(11)	C0AA	O3	Gd1^1	126.9(3)
O1^1	Gd1	O2L	124.89(10)	C5	O5	C5^5	118.0(4)
O1	Gd1	O2L	150.27(10)	O6	S1	O7	112.77(19)
O1^2	Gd1	O2L	138.59(10)	O6	S1	C4	105.56(17)
O1	Gd1	O1L	76.92(10)	O6	S1	O4	112.67(18)

O1[1]	Gd1	O1L	131.51(10)	O7	S1	C4	107.59(18)
O1	Gd1	O4[3]	105.10(9)	O7	S1	O4	110.83(18)
O3[4]	Gd1	O1[1]	74.09(10)	O4	S1	C4	106.99(17)
O3[4]	Gd1	O1	99.46(10)	C5	C4	S1	119.1(3)
O3[4]	Gd1	O1[2]	144.75(10)	C3	C4	S1	121.5(3)
O3[4]	Gd1	O2L	67.64(10)	C3	C4	C5	119.4(4)
O3[4]	Gd1	O1L	75.10(12)	O3	C0AA	C2AA	117.3(4)
O3[4]	Gd1	O4[3]	138.02(10)	O3	C0AA	O2	124.6(4)
O2	Gd1	O1[2]	78.91(10)	O2	C0AA	C2AA	118.1(4)
O2	Gd1	O1[1]	82.15(10)	C7	C2AA	C0AA	118.8(3)
O2	Gd1	O1	142.13(11)	C7	C2AA	C3	119.8(3)
O2	Gd1	O3[4]	99.87(11)	C3	C2AA	C0AA	121.3(3)
O2	Gd1	O2L	67.60(11)	C6	C7	C2AA	120.7(4)
O2	Gd1	O1L	139.78(11)	C7	C6	C5	119.2(3)
O2	Gd1	O4[3]	80.86(10)	O5	C5	C4	117.8(3)
O1L	Gd1	O1[2]	127.77(10)	O5	C5	C6	120.9(3)
O1L	Gd1	O2L	73.90(11)	C6	C5	C4	121.0(3)
O4[3]	Gd1	O1[2]	77.01(9)	C4	C3	C2AA	119.8(4)
O4[3]	Gd1	O1[1]	145.91(10)	C0AA	O2	Gd1	137.1(3)
O4[3]	Gd1	O2L	74.32(10)	S1	O4	Gd1[6]	145.88(17)
O4[3]	Gd1	O1L	77.97(11)	N10	C9	C1	144(3)
Gd1	O1	Gd1[2]	112.51(11)				

[1]-1/2-y,1/2+x,-1/2-z; [2]-1-x,-y,+z; [3]-1-y,1+x,-1-z; [4]-1/2+y,-1/2-x,-1/2-z; [5]-2-x,-1-y,+z; [6]-1+y,-1-x,-1-z

CP 2

Atom	Atom	Atom	Angle/°	Atom	Atom	Atom	Angle/°
O1	Dy1	O1[1]	72.60(11)	Dy1	O1	Dy1[2]	112.17(12)
O1[1]	Dy1	O1[2]	70.92(11)	Dy1	O1	Dy1[4]	105.07(10)
O1	Dy1	O1[2]	66.97(12)	C0AA	O3	Dy1[1]	128.0(3)
O1[2]	Dy1	O2L	139.52(11)	C5[5]	O5	C5	118.6(4)
O1	Dy1	O2L	149.23(11)	O6	S1	C4	105.59(18)
O1[1]	Dy1	O2L	124.55(10)	O6	S1	O4	112.59(18)
O1	Dy1	O1L	76.72(11)	O7	S1	O6	112.8(2)
O1[1]	Dy1	O1L	131.94(11)	O7	S1	C4	107.30(18)
O1	Dy1	O4[3]	105.59(10)	O7	S1	O4	110.95(19)
O3[4]	Dy1	O1[2]	144.63(9)	O4	S1	C4	107.12(18)
O3[4]	Dy1	O1	99.01(11)	C5	C4	S1	118.9(3)
O3[4]	Dy1	O1[1]	73.92(10)	C3	C4	S1	121.6(3)

O3^{4}	Dy1	O2L	67.01(11)	C3	C4	C5	119.5(4)
O3^{4}	Dy1	O1L	75.45(12)	O3	C0AA	C2AA	117.6(4)
O3^{4}	Dy1	O4^{3}	138.28(10)	O3	C0AA	O2	124.0(4)
O2	Dy1	O1^{2}	79.80(11)	O2	C0AA	C2AA	118.4(4)
O2	Dy1	O1	143.39(11)	C7	C2AA	C0AA	118.7(4)
O2	Dy1	O1^{1}	82.62(10)	C3	C2AA	C0AA	121.8(4)
O2	Dy1	O3^{4}	99.50(12)	C3	C2AA	C7	119.4(4)
O2	Dy1	O2L	67.38(12)	C6	C7	C2AA	120.7(4)
O2	Dy1	O1L	138.74(12)	C5	C6	C7	118.9(4)
O2	Dy1	O4^{3}	80.15(10)	O5	C5	C4	117.9(3)
O1L	Dy1	O1^{2}	127.53(11)	O5	C5	C6	120.8(4)
O1L	Dy1	O2L	73.29(12)	C6	C5	C4	121.1(4)
O4^{3}	Dy1	O1^{1}	145.59(10)	C4	C3	C2AA	120.2(4)
O4^{3}	Dy1	O1^{2}	76.84(9)	C0AA	O2	Dy1	135.9(3)
O4^{3}	Dy1	O2L	74.83(11)	S1	O4	Dy1^{6}	145.38(19)
O4^{3}	Dy1	O1L	78.07(11)	N10	C9	C1	147(3)
Dy1^{4}	O1	Dy1^{2}	102.12(10)				

^{1}-1/2-y,1/2+x,-1/2-z; ^{2}-1-x,-y,+z; ^{3}-1-y,1+x,-1-z; ^{4}-1/2+y,-1/2-x,-1/2-z; ^{5}-2-x,-1-y,+z; ^{6}-1+y,-1-x,-1-z

CP**3**

Atom	**Atom**	**Atom**	**Angle/°**	**Atom**	**Atom**	**Atom**	**Angle/°**
O1	Ho1	O1^{1}	72.47(13)	Ho1	O1	Ho1^{2}	112.21(12)
O1^{1}	Ho1	O1^{2}	71.04(12)	Ho1	O1	Ho1^{4}	104.84(12)
O1	Ho1	O1^{2}	66.92(12)	C0AA	O3	Ho1^{1}	127.2(3)
O1^{2}	Ho1	O2L	138.94(12)	C5^{5}	O5	C5	118.5(6)
O1	Ho1	O2L	149.76(12)	O6	S1	C4	105.5(2)
O1^{1}	Ho1	O2L	124.64(12)	O6	S1	O4	112.6(2)
O1	Ho1	O1L	76.90(13)	O7	S1	O6	112.8(2)
O1^{1}	Ho1	O1L	131.74(13)	O7	S1	C4	107.4(2)
O1	Ho1	O4^{3}	105.57(12)	O7	S1	O4	111.1(2)
O3^{4}	Ho1	O1^{2}	144.76(12)	O4	S1	C4	107.0(2)
O3^{4}	Ho1	O1	99.36(12)	C5	C4	S1	119.3(4)
O3^{4}	Ho1	O1^{1}	73.89(12)	C3	C4	S1	121.6(4)
O3^{4}	Ho1	O2L	67.22(13)	C3	C4	C5	119.2(5)
O3^{4}	Ho1	O1L	75.41(14)	O3	C0AA	C2AA	117.0(5)
O3^{4}	Ho1	O4^{3}	137.86(13)	O2	C0AA	O3	124.7(5)
O2	Ho1	O1^{2}	79.50(12)	O2	C0AA	C2AA	118.3(5)
O2	Ho1	O1	143.00(12)	C7	C2AA	C0AA	119.2(5)

O2	Ho1	O1[1]	82.55(12)	C7	C2AA	C3	119.2(5)
O2	Ho1	O3[4]	99.36(13)	C3	C2AA	C0AA	121.4(5)
O2	Ho1	O2L	67.24(13)	C2AA	C7	C6	121.1(5)
O2	Ho1	O1L	138.96(14)	C5	C6	C7	118.8(5)
O2	Ho1	O4[3]	80.45(13)	O5	C5	C4	117.7(4)
O1L	Ho1	O1[2]	127.71(13)	O5	C5	C6	120.9(4)
O1L	Ho1	O2L	73.53(14)	C6	C5	C4	121.2(4)
O4[3]	Ho1	O1[1]	146.07(11)	C4	C3	C2AA	120.4(5)
O4[3]	Ho1	O1[2]	77.10(11)	C0AA	O2	Ho1	136.0(3)
O4[3]	Ho1	O2L	74.32(13)	S1	O4	Ho1[6]	146.0(2)
O4[3]	Ho1	O1L	77.84(14)	N10	C9	C1AA	148(3)
Ho1[4]	O1	Ho1[2]	102.33(12)				

[1]1/2-y,-1/2+x,1/2-z; [2]1-x,-y,+z; [3]1-y,-1+x,1-z; [4]1/2+y,1/2-x,1/2-z; [5]2-x,1-y,+z; [6]1+y,1-x,1-z

CP **4**

Atom	**Atom**	**Atom**	**Angle/°**	**Atom**	**Atom**	**Atom**	**Angle/°**
O1	Er1	O1[1]	72.59(14)	Er1	O1	Er1[4]	104.94(13)
O1	Er1	O1[2]	66.99(12)	Er1[4]	O1	Er1[2]	102.21(13)
O1[1]	Er1	O1[2]	71.03(14)	C0AA	O3	Er1[1]	127.7(3)
O1[1]	Er1	O2L	124.35(14)	C5[5]	O5	C5	117.9(6)
O1	Er1	O2L	149.15(13)	O6	S1	O7	112.5(3)
O1[2]	Er1	O2L	139.70(12)	O6	S1	C4	105.9(2)
O1	Er1	O1L	76.60(13)	O6	S1	O4	112.8(3)
O1[1]	Er1	O1L	131.99(14)	O7	S1	C4	107.0(3)
O1	Er1	O4[3]	105.81(13)	O7	S1	O4	111.0(2)
O3[4]	Er1	O1[1]	73.88(13)	O4	S1	C4	107.3(2)
O3[4]	Er1	O1	99.17(13)	C5	C4	S1	119.2(4)
O3[4]	Er1	O1[2]	144.72(14)	C3	C4	S1	121.2(4)
O3[4]	Er1	O2L	66.62(14)	C3	C4	C5	119.6(5)
O3[4]	Er1	O1L	75.80(16)	O3	C0AA	C2AA	117.1(5)
O3[4]	Er1	O4[3]	138.12(13)	O3	C0AA	O2	124.5(5)
O2	Er1	O1[2]	80.07(12)	O2	C0AA	C2AA	118.3(5)
O2	Er1	O1[1]	82.77(13)	C7	C2AA	C0AA	119.2(5)
O2	Er1	O1	143.65(13)	C7	C2AA	C3	118.7(4)
O2	Er1	O3[4]	99.11(14)	C3	C2AA	C0AA	122.0(5)
O2	Er1	O2L	67.20(14)	C2AA	C7	C6	120.7(5)
O2	Er1	O1L	138.61(14)	C5	C6	C7	119.5(5)
O2	Er1	O4[3]	80.00(14)	O5	C5	C4	117.8(5)
O1L	Er1	O1[2]	127.25(14)	C6	C5	O5	121.2(4)

[1]1/2-y,-1/2+x,1/2-z; [2]1-x,-y,+z; [3]1-y,-1+x,1-z; [4]1/2+y,1/2-x,1/2-z; [5]2-x,1-y,+z; [6]1+y,1-x,1-z

Channel analysis

To establish a structure-property relationship especially to indirectly support the Grotthuss mechanism of proton conduction, channel analysis was carried out on CP **4** as a representative model using the software package ToposPro.

.

When analyzing the channels in the framework, intra-channel species can be removed in two ways and hence two different frameworks can be obtained for analysis. The first framework (I) corresponds to a structure, from which only solvate water and acetonitrile molecules have been removed. If both solvate molecules and coordinated water molecules are removed, then the second framework (II) is obtained. The dimensionality of the void space and channel descriptors were determined by means of Voronoi polyhedral (Table S7). The migration map is shown in Fig. S23.

Table S7. The widest periodic channel systems without solvent (I) or without solvent and coordinated water molecules (II)

Framework	***Total porosity***	R_i	***Periodicity***	R_f	R_{if}	***Direction***	***Z***
I	43	3.0	1	0.5	3.0	(0, 0, 1)	2
II	50	3.5	1	0.7	3.5	(0, 0, 1)	2

Z – number of channels system in the unit cell; ***Periodicity*** –periodisity of a channels system; ***Direction*** – vector of direction one-periodic channels system or vector of normal to two-periodic channels system; ***Total Porosity*** – percent of empty space in a structure, calculeted by formula $(V_{cell} - V_{vdw})/V_{cell}$ *100%; ***Radius of largest included sphere (R_i)*** – the radius of most largest spherical probe that can be included in a structure without intersection with van-der-Waals surface of the structure (Å); ***Radius of largest free sphere (R_f)***– the radius of most largest spherical probe that can free migrate in a given channels system of a structure (Å); ***Radius of largest included free sphere (R_{if})*** – the radius of most largest spherical probe that can be included in a given channels system of a structure (Å).

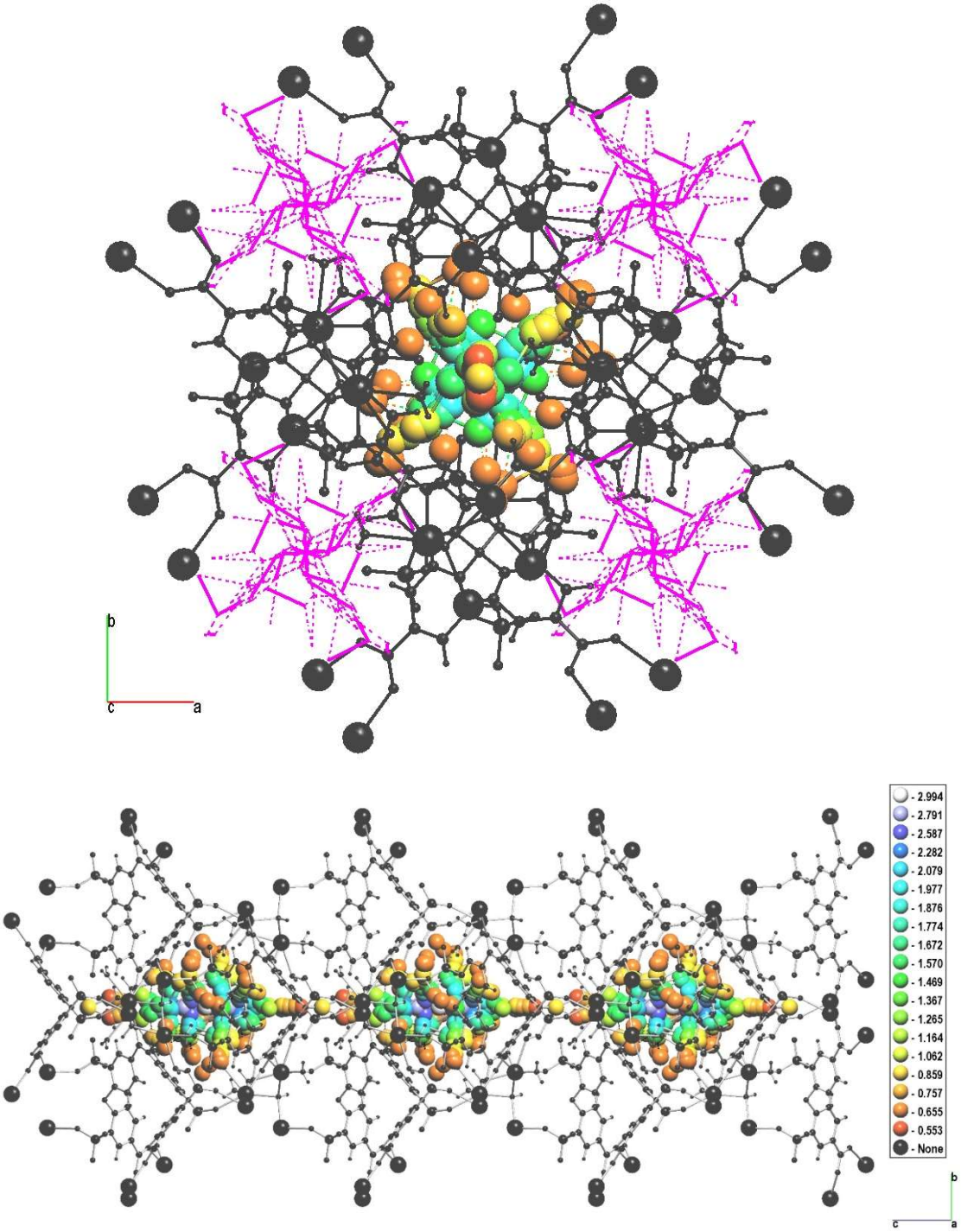

Fig. S23 One-periodic migration map for framework I in [001] (top) and [100] (bottom) projections. Atoms are displayed in black. The color of the voids determines the minimum distance to the van der Waals surface of the nearest atoms. The legend of the coloring is on the right.

The possibility of migration of the H_3O^+ cation in the framework is determined by the radius of the largest free sphere $\boldsymbol{R_f}$. If the kinetic radius of the H_3O^+ cation is taken into account, which is *ca.* 1.6 Å [S. S. Park, A. J. Rieth, C. H. Hendon and M. Dincă, *J. Am. Chem. Soc.*, 2018, **140**, 2016-2019.], then the H_3O^+ cation cannot migrate through the channels. The radius $\boldsymbol{R_f}$ = 0.5-0.7 Å is much less than the size required. Hence, the channel analysis precludes the possibility of physical diffusion of the proton carrying unit (i.e., hydronium ions) in the channel through vehicle mechanism, thereby indirectly supporting the Grotthuss mechanism of proton conduction.